# Electron Microscopic Analysis of Hippocampal Axo-Somatic Synapses in a Chronic Stress Model for Depression

Dávid Csabai,[1] László Seress,[2] Zsófia Varga,[1] Hajnalka Ábrahám,[2,3] Attila Miseta,[4] Ove Wiborg,[5] and Boldizsár Czéh[1,4,5]*

**ABSTRACT:** **Stress can alter the number and morphology of excitatory synapses in the hippocampus, but nothing is known about the effect of stress on inhibitory synapses. Here, we used an animal model for depression, the chronic mild stress model, and quantified the number of perisomatic inhibitory neurons and their synapses. We found reduced density of parvalbumin-positive (PV+) neurons in response to stress, while the density of cholecystokinin-immunoreactive (CCK+) neurons was unaffected. We did a detailed electron microscopic analysis to quantify the frequency and morphology of perisomatic inhibitory synapses in the hippocampal CA1 area. We analyzed 1100 CA1 pyramidal neurons and 4800 perisomatic terminals in five control and four chronically stressed rats. In the control animals we observed the following parameters: Number of terminals/soma = 57; Number of terminals/100 μm cell perimeter = 10; Synapse/terminal ratio = 32%; Synapse number/100 terminal = 120; Average terminal length = 920nm. None of these parameters were affected by the stress exposure. Overall, these data indicate that despite the depressive-like behavior and the decrease in the number of perisomatic PV+ neurons in the light microscopic preparations, the number of perisomatic inhibitory synapses on CA1 pyramidal cells was not affected by stress. In the electron microscope, PV+ neurons and the axon terminals appeared to be normal and we did not find any apoptotic or necrotic cells. This data is in sharp contrast to the remarkable remodeling of the excitatory synapses on spines that has been reported in response to stress and depressive-like behavior.** © 2016 The Authors Hippocampus Published by Wiley Periodicals, Inc.

**KEY WORDS:** **inhibitory synapse; hippocampus; parvalbumin; synaptic density; ultrastructure**



[1] **MTA – PTE, Neurobiology of Stress Research Group, Szentágothai Research Center, Pécs, 7624, Hungary;** [2] **Central Electron Microscope Laboratory, University of Pécs, Medical School, Pécs, 7624, Hungary;** [3] **Department of Medical Biology, University of Pécs, Medical School, Pécs, 7624, Hungary;** [4] **Department of Laboratory Medicine, University of Pécs, Medical School, Pécs, 7624, Hungary;** [5] **Translational Neuropsychiatry Unit, Department of Clinical Medicine, Aarhus University, Risskov, Denmark**

Grant sponsor: Lundbeck Foundation; Grant number: R83-A7631; Grant sponsor: Hungarian Brain Research Program "B"; Grant number: KTIA_NAP_13-2-2014-0019.

Abbreviations: CCK, cholecystokinin; CMS, chronic mild stress; PV+, parvalbumin-positive; sIPSCs, spontaneous inhibitory postsynaptic currents

*Correspondence to: Boldizsár Czéh, MD, PhD, DSc, Institute of Laboratory Medicine, Faculty of Medicine, University of Pécs, H-7624 Pécs, Ifjúság út 13. Hungary. E-mail: czeh.boldizsar@pte.hu

Accepted for publication 23 August 2016.
DOI 10.1002/hipo.22650
Published online 29 August 2016 in Wiley Online Library (wileyonlinelibrary.com).

## INTRODUCTION

Stress can affect the cellular integrity and functioning of the hippocampus (reviewed by Lucassen et al., 2014; McEwen et al., 2015). Cellular studies report on reduced apical dendritic complexity of pyramidal neurons and reduced density of dendritic spines (Watanabe et al., 1992; Magarinos et al., 1996; Pawlak et al., 2005; Leuner and Shors, 2013). Electron microscopic studies proved that stress results in structural remodeling and loss of axo-spinous synapses (Magarinos et al., 1997; Sandi et al., 2003; Pawlak et al., 2005; Stewart et al., 2005; Donohue et al., 2006; Hajszan et al., 2009; Sousa et al., 2000; Maras et al., 2014). These synaptic alterations have been supported by electrophysiological studies showing disturbed excitatory synaptic neurotransmission in chronically stressed animals (Krugers et al., 2010; Kallarackal et al., 2013; Timmermans et al., 2013). Furthermore, such stress-induced alterations of the glutamatergic synapses have been suggested to play a key role in the pathophysiology of mood disorders (Popoli et al., 2011; Duman, 2014; Thompson et al., 2015).

It is extensively documented that stress and stress-hormones influence GABAergic signaling in the hippocampus (Mody and Maguire, 2012; MacKenzie and Maguire, 2013; Maguire, 2014), but little is known on the stress-induced structural changes affecting the GABAergic network. There are reports on altered inhibitory neurotransmission and reduced number of GABAergic cells in chronically stressed animals (Czéh et al., 2005, 2015; Gronli et al., 2007; Harte et al., 2007; Hu et al., 2010, 2011; Holm et al., 2011; MacKenzie and Maguire, 2015; Lee et al., in press). Several studies focused on parvalbumin-positive (PV+) basket cells and documented that different stress protocols can reduce their numbers in all hippocampal subareas (Czéh et al., 2005, 2015; Harte et al., 2007; Hu et al., 2010; Filipovic et al., 2013; Milner et al., 2013; Godavarthi et al., 2014; Megahed et al., 2015, reviewed by Zaletel et al., 2016). One of these studies also found histopathological indications of neuronal degeneration and cell death in the hilar region of chronically stressed rats (Milner et al., 2013). This finding raised the possibility that PV+ neurons may die in response to chronic stress.

Parvalbumin-containing neurons represent a major subpopulation of GABAergic cells in the neocortex and hippocampus (Ribak et al., 1990; Freund and Buzsaki, 1996; Markram et al., 2004). Interneurons are classified based on the target structure of their axon-terminals. According to this classification PV-containing cells are perisomatic inhibitory neurons. As perisomatc inhibitory cells, they form symmetric synapses on the cell soma, proximal dendrites and axon initial segments of the popstsynaptic neurons (Kosaka et al, 1987; Ribak et al, 1990; Freund and Buzsaki, 1996). Perisomatic interneurons account for nearly 50% of all hippocampal interneurons (Freund and Buzsaki, 1996), and can be further divided into two separate subgroups according to their expression of cellular markers cholecystokinin (CCK) and PV (Freund and Katona, 2007; Whissell et al, 2015).

In our earlier papers, we discussed that the stress-induced decrease in the number of PV-containing interneurons may indicate either a real excitotoxic cell loss or that the intracellular PV content of the cells is reduced below levels detectable by immunocytochemistry (Czéh et al., 2005, 2015). But so far, neither possibility has been unambiguously proven. We hypothesized that if PV+ perisomatic neurons die then, the number of their perisomatic synapses should also decrease. Therefore, we set out to make a new experiment with the aim to confirm the previous findings on stress-induced reduction of perisomatic inhibitory neurons and to investigate what happens with their perisomatic inhibitory synapses. We subjected rats to a similar chronic stress protocol as earlier and quantified PV+ and CCK+ neurons at the light microscopic level and then, their axo-somatic synapses on the CA1 pyramidal neurons at the electron microscopic level. We focused on the PV+ and CCK+ neurons because these two cellular markers identify the entire population of the perisomatic inhibitory neurons (Freund and Katona, 2007; Whissell et al, 2015).

## MATERIALS AND METHODS

### Ethics

All animal experiments were conducted in accordance with NIH guidelines and were accepted by the Danish National Committee Ethics in Animal Experimentation (2008/561–477).

### Animals

Adult male Wistar rats (5-6 weeks old, with a body weight of about 120g) were obtained from Taconic (Denmark). Nine rats were used in the present study: $n = 5$ controls and $n = 4$ stressed. These nine animals were selected from a much larger cohort of animals that were all subjected to the same experimental procedures. We selected the four stressed animals based on their pronounced anhedonic behaviors (the behavioral phenotyping of the animals is described below). The animals were singly housed, except when grouping was applied as a stress parameter. Food and water was available *ad libitum* except when food and/or water deprivation was applied as a stress parameter. The standard 12-h light/dark cycle was only changed in course of the stress regime.

### Behavioral Phenotyping

Animals phenotyped with the use of the sucrose consumption test to detect their hedonic-anhedonic behavior in response to stress. The protocol of the sucrose consumption test has been described in detail previously (Henningsen et al., 2012). Briefly, all animals were trained to consume a palatable sucrose solution (1.5%). The training lasted for five weeks, with sucrose test conducted twice a week during the first two weeks and once a week during the last three weeks. Animals were food and water deprived 14 h before the test, which was performed by free access to a bottle with sucrose solution for 1 h. During the entire stress period, the sucrose consumption test was performed once a week. Baseline sucrose consumption was defined as the mean sucrose consumption during three sucrose tests conducted before stress initiation.

### An Animal Model for Depression: The Chronic Mild Stress (CMS) Protocol

The CMS is a realistic and one of the most thoroughly validated animal models for depression (Willner et al., 1992, reviewed by Willner, 2005; Wiborg, 2013). The CMS procedure has been described in detail in our earlier publications (Henningsen et al., 2009, 2012; Wiborg, 2013; Czéh et al., 2015). Briefly, 12-weeks old rats were divided into two matched groups on the basis of their baseline sucrose intake, and housed in separate rooms. One group of rats was exposed to 9 weeks of mild stressors. A second group of rats (controls) was left undisturbed. The schedule of the CMS was: a period of intermittent illumination, stroboscopic light, grouping, food or water deprivation; two periods of soiled cage and no stress; and three periods of 45° cage tilting (Table 1). During grouping, rats were housed in pairs with different partners, with the individual rat alternately being a resident or an intruder. All the stressors lasted from 10 to 14 hours. Based on the sucrose consumption, the hedonic state of the animals was evaluated and stressed rats were divided into stress sensitive rats (anhedonic animals) and resilient rats (Henningsen et al., 2012). Anhedonic animals are the ones that reduce their sucrose solution intake by more than 30% in response to stress.

### Perfusion, Brain Tissue Preparation, and Immunohistochemistry Labeling

After an overdose of sodium pentobarbital (200 mg/ml dissolved in 10% ethanol) animals were transcardially perfused with ice cold 0.9% physiological saline followed by 4% paraformaldehyde containing 0.2% glutaraldehyde in 0.1 M phosphate buffer (pH 7.4). The brains were removed and postfixed overnight in the same solution at 4°C, but without

*TABLE 1.*

*The Weekly Schedule of the CMS Protocol*

| | Daytime | Evening |
|---|---|---|
| **Monday** | Intermittent illumination | No stress |
| **Tuesday** | Water deprivation | Cage tilting |
| **Wednesday** | Strobe flashing | Wetting |
| **Thursday** | No stress | Food and water deprivation |
| **Friday** | Sucrose test | Grouping |
| **Saturday** | Food and water deprivation | Cage tilting |
| **Sunday** | Cage tilting | Wetting |

Every micro-stressor lasted for 10-14 hours.
Intermittent illumination: light on/off every 2 h; Cage tilting into a 45° position; Strobe flashing: stroboscopic lightning; Wetting: pouring water into the cage to damp bedding; Grouping: pairing two rats by having an unfamiliar partner at each grouping session.

glutaraldehyde. Serial, 80 μm thick, coronal sections were cut using a Vibratome (Leica VT1200 S) throughout the entire hippocampal formation along the septo-temporal axis (from −1.60 to −6.30 relative to Bregma, (Paxinos and Watson, 1998). Sections for the electron microscopic analysis were transferred to graded sucrose solutions (15%–30% in PB, pH 7.0–7.4) for cryo-protection and stored at 4°C until they sank. After this procedure, sections were frozen over liquid nitrogen and thawed for three times to increase antibody penetration.

### *Light microscopy*

Immunolabeling was carried out to visualize parvalbumin-immunoreactive and cholecystokinin-immunoreactive neurons according to our standard immunohistochemistry protocol (Czéh et al., 2015). Free-floating sections from the control and stress groups were always processed in parallel to avoid any nonspecific effect of the staining procedure. Briefly the main steps: 1% $H_2O_2$ pretreatment; incubation with 5% normal goat serum (Vector Laboratories); one night incubation with either monoclonal anti-parvalbumin antibody (1:10 000, Swant, Cat #: 235), or with polyclonal anti-cholecystokinin-8 antibody (1:5000, AbCam, Cat #: ab43842). The immunereaction was visualized by incubation with a corresponding biotinylated secondary antibody (1:200; Vector Laboratories), followed by incubation with avidin-biotin-horseradish peroxidase (1:200; Vectastaine Elite ABC Kit, Vector) and development with DAB (1:200; DAB Peroxidase Substrate Kit, Vector).

### *Electron microscopy*

Sections for the electron microscopic analysis were immune-labeled as described above except that we omitted the use of Triton X-100 during the staining protocol. After the immune-staining sections were osmicated (1% $OsO_4$ in PB for 30 min), dehydrated in graded ethanol (the 70% ethanol contained 1% uranyl acetate). After complete dehydration in ascending ethanol series, sections were immersed in propylene-oxide, then into a mixture of propylene-oxide and Durcupan resin then, were flat-embedded in Durcupan resin (Fluka-Sigma-Aldrich, Hungary). After polymerization at 56°C for 48 hours, the sections were viewed under a light microscope, and areas of interest were chosen for re-embedding and electron microscopic sectioning. To select the appropriate region of the CA1 area for the ultrathin sectioning, semithin (500nm) sections were stained with toluidine blue. Ultrathin (60nm) sections were cut with a Leica Ultracut UCT microtome and collected on Formvar-coated single slot copper grids, stained with uranyl-acetate and lead citrate and examined with a JEOL 1200 EX-II electron microscope.

## Quantitative Analysis of Neuron Numbers and Their Perisomatic Synapses

### *Light microscopic analysis*

We determined the neuronal density of PV+ and CCK+ neurons in the dorsal hippocampus. We did a systematic and random sampling for the cell counting. The sampling was systematic because we collected every coronal section between Bregma points of −1.60 and −5.80 according to the atlas of Paxinos and Watson (1998). Neuronal densities were determined in this frontal portion of the hippocampus which contains almost the entire dorsal hippocampus. From this complete series of 80 μm thick sections we selected two series of sections with always equal, 400 μm intervals between them ($n = 8$–10 sections/series). One of these two series of sections was stained for PV+ neurons and the other series of sections was stained for CCK+ neurons. The sampling was also random because the starting point for the section series was random, ±150 μm from the Bregma point of −1.60 (Paxinos and Watson, 1998). Neurons were counted in every different hippocampal subarea (dentate gyrus, CA2-3, CA1) separately using the Neurolucida Version 7 reconstruction system (MicroBrightField, Williston, VT, USA). First the contours of the different hippocampal areas and layers were traced under low magnification and then the cells were examined and counted using an objective of 20× magnification, omitting labeled profiles in the outermost focal plane. We report here the neuron numbers as numerical densities (neuron densities), which we calculated based on the following formula: the number of counted cells was divided by the volume of the traced hippocampal area and expressed as cell number/$mm^3$ volume.

### *Electron microscopic analysis*

We analyzed and quantified the axo-somatic synapses projecting onto CA1 pyramidal cell bodies in the dorsal hippocampus. Perisomatic terminals were identified with 20,000× magnification based on their pre- and post-synaptic density, the presence of the rather oval vesicles and the synaptic cleft between the pre- and post-synaptic membranes. The goniometer tilt was used to get clear identification of the synapses.

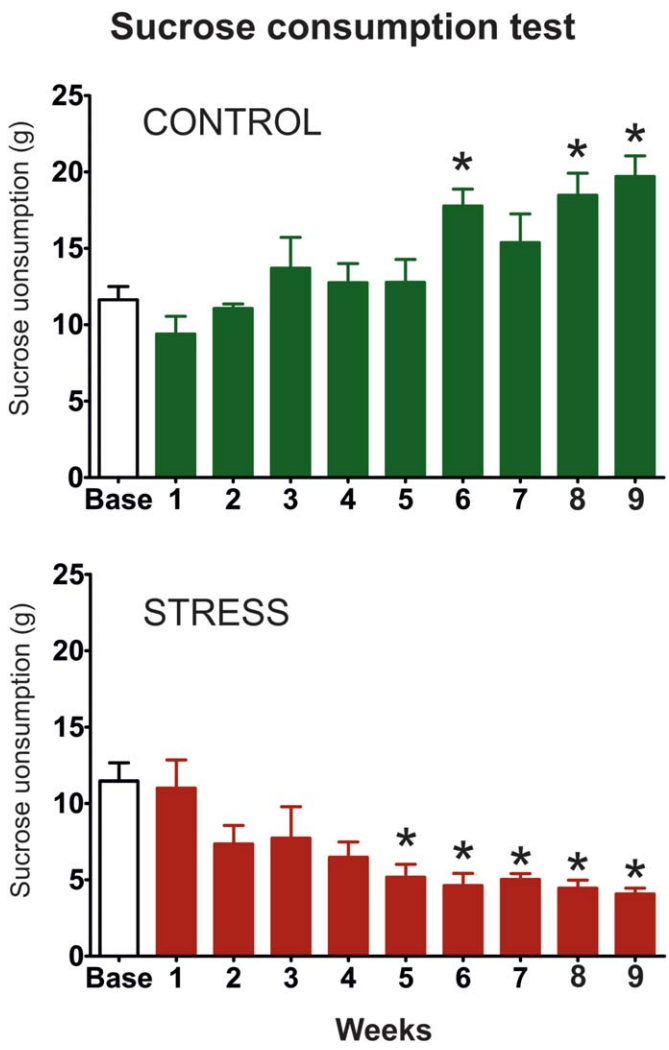


**FIGURE 1. The graphs display the sucrose consumption data of the animals that were used for the quantitative histopathological and electron microscopic analysis. The sucrose consumption test was used to demonstrate the hedonic-anhedonic behavior of the animals. Control rats gradually increased their sucrose intake indicating a healthy hedonic behavior. In contrast, the stressed animals progressively reduced their sucrose which indicates anhedonic behavior. Since anhedonia is a core feature of depression thus, this test demonstrates the depressive-like behavior of the animals. The baseline sucrose consumption was defined as the mean sucrose consumption during three sucrose tests conducted before stress initiation. Statistics: one-way ANOVA, followed by Dunnets's multiple comparison test in which the results are compared to the baseline consumption of the same group. *$P < 0.05$, versus the baseline value of the same group. [Color figure can be viewed at wileyonlinelibrary.com]**

Symmetric synapses on the somata of the pyramidal neurons were counted. Pyramidal neurons do not receive asymmetric axo-somatic synapses. Within the pyramidal layer, 1–2% of neurons received both asymmetric and symmetric axosomatic synapses. These cells were local circuit neurons and were not included in this study. Neurons in the strata oriens and radiatum were not included in this study. Neuronal perimeter, synaptic membrane length as opposed to the soma, number of active zones and membrane length of the axo-somatic terminals were also analyzed. For these examinations 5000× – 50000× magnification images were taken from the pyramidal cell layer of the CA1 region and were evaluated with Olympus iTEM software.

### Statistical Analysis

In all cases when we calculated quantitative data, '*n*' was the number of animals. Results are presented as the mean ± SEM. The data on neuron numbers and synaptic morphology and numbers were analyzed with two-tailed unpaired *t*-test. Results of the sucrose preference test were analyzed with repeated measures of one-way ANOVA, followed by Dunnets's Multiple Comparison Test.

## RESULTS

### Chronic Stress-Induced Depressive-Like Behavior

The sucrose consumption test was used to evaluate the hedonic-anhedonic behavior of the animals. Nine weeks of CMS resulted in significantly decreased sucrose consumption indicating anhedonic, depressive-like behavior in the stressed animals. Figure 1 displays the sucrose intake data of the rats that were used for the subsequent histopathological analysis. One-way ANOVA followed by Dunnets's multiple comparison test demonstrated that control rats consumed significantly more sucrose on week 6 ($q = 3.73$, $P < 0.01$), 8 ($q = 4.18$, $P < 0.01$) and 9 ($q = 4.98$, $P < 0.001$) compared to their own baseline. A similar statistical analysis demonstrated that the stressed rats consumed significantly less sucrose from the stress week 5 onwards compared to their own baseline (Fig. 1). The results of the statistical comparisons were: week 5 ($q = 3.65$, $P < 0.01$), week 6 ($q = 4.04$, $P < 0.01$), week 7 ($q = 3.75$, $P < 0.01$), week 8 ($q = 4.16$, $P < 0.01$) and week 9 ($q = 4.42$, $P < 0.01$).

### Quantitative Light Microscopic Analysis of the Perisomatic Inhibitory Neurons

We stained and quantified the two subpopulations of perisomatic inhibitory neurons, the PV+ and CCK+ cells, in the dorsal hippocampus. These two cellular markers label the entire population of the perisomatic inhibitory neurons. Representative photomicrographs of the PV and CCK immunohistochemistry labelings are shown on Figure 2.

In the dorsal hippocampi of control rats, we observed the following PV+ cell densities: in the dentate gyrus 1650 ± 160 neurons/mm$^3$; in the CA2-3 areas 2950 ± 230 neurons/mm$^3$ and in the CA1 area 3120 ± 215 neurons/mm$^3$. Stress reduced the density of PV+ neurons in all these hippocampal subareas (Fig. 3A). In the dentate gyrus, PV+ cell densities were reduced by 33% to 1110 ± 75 neurons/mm$^3$ ($t = 3.22$,

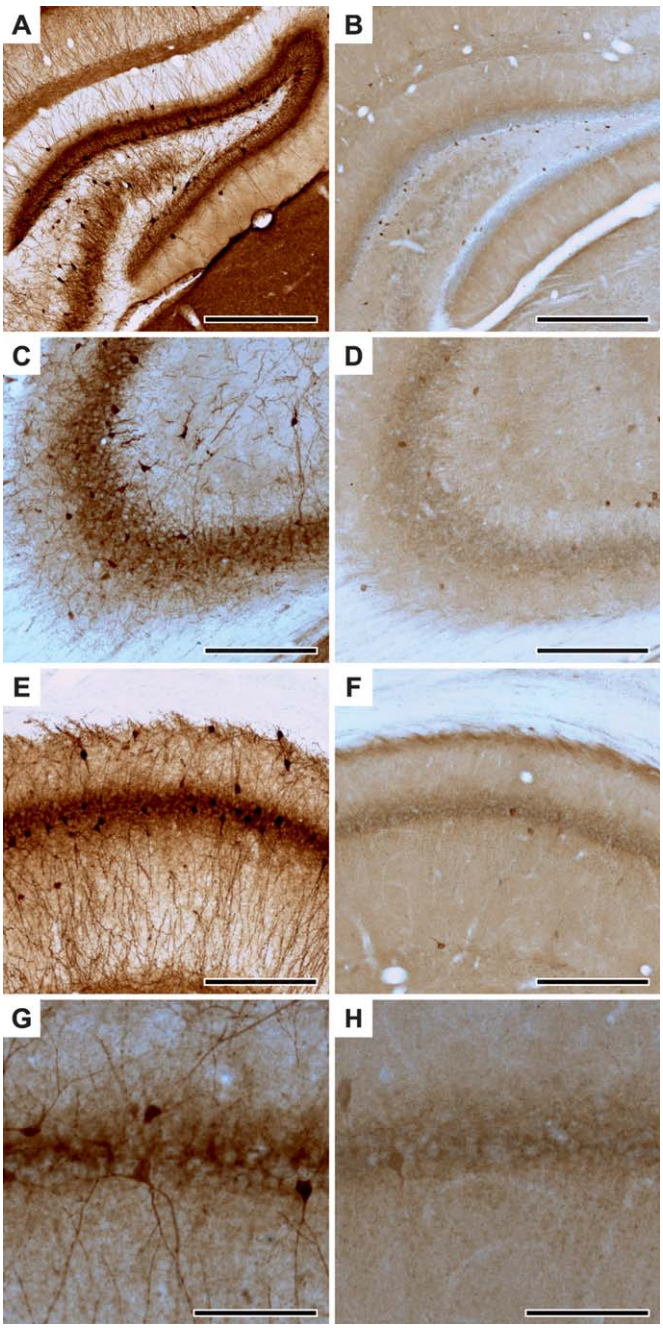


**FIGURE 2. Representative photomicrographs of parvalbumin- and cholecystokinin-immunoreactive neurons in the dorsal hippocampus. PV+ neurons in the dentate gyrus (A), CA3 (C) and CA1 areas (E, G). CCK+ neurons in the dentate gyrus (B), CA3 (D) and CA1 areas (F, H). Panels G and H show high magnification images of PV+ (G) and CCK+ (H) interneurons projecting to the CA1 pyramidal cell layer. Scale bars: 250 μm for A-F and 100 μm for G-H. [Color figure can be viewed at wileyonlinelibrary.com]**

$P < 0.01$). In the CA2-3 areas, PV+ cell densities were reduced by 20% to $2390 \pm 65$ neurons/mm$^3$ ($t = 2.48$, $P < 0.05$) and in the CA1 area, PV+ cell densities were reduced by 22% to $2420 \pm 175$ neurons/mm$^3$ ($t = 2.54$, $P < 0.01$).

The CCK+ neurons were much fewer in number. We detected the following CCK+ neuronal densities in the dorsal hippocampus of the control rats: in the dentate gyrus $870 \pm 50$ neurons/mm$^3$; in the CA2-3 areas $1320 \pm 50$ neurons/mm$^3$ and in the CA1 area $1090 \pm 25$ neurons/mm$^3$. These CCK+ neuronal densities were unaffected by the stress (Fig. 3B).

## Quantitative Electron Microscopic Analysis of the Axo-Somatic Synapses

As it is shown in Figure 4A blocks of the CA1 area were cut from two selected dorsal hippocampal sections after PV immunohistochemistry and re-embedded for electron microscopy. Examples of representative electron microscopic electron

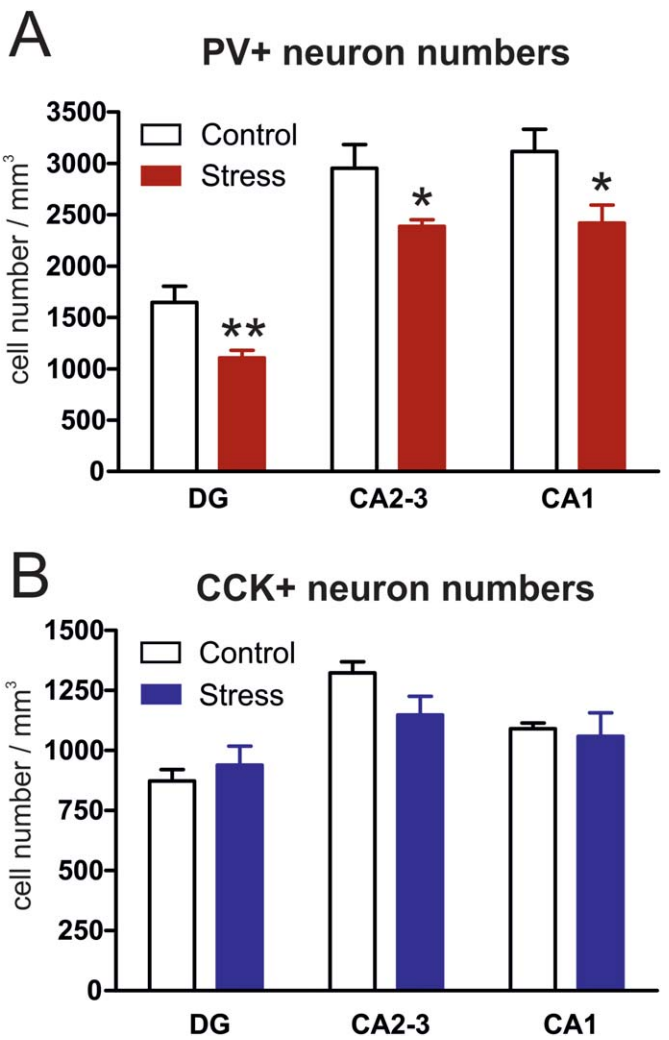


**FIGURE 3. The effect of stress on the number of perisomatic inhibitory neurons in the dorsal hippocampus. The two major subpopulations of perisomatic inhibitory neurons were quantified: (A) parvalbumin+ and (B) cholecystokinin+ neurons. Note that stress significantly reduced the number of PV+ neuron numbers in all hippocampal subareas, while CCK+ neurons were not affected by stress. Statistical analysis: two-tailed unpaired *t*-test. *$P < 0.05$, **$P < 0.01$, *versus* the Control group. [Color figure can be viewed at wileyonlinelibrary.com]**

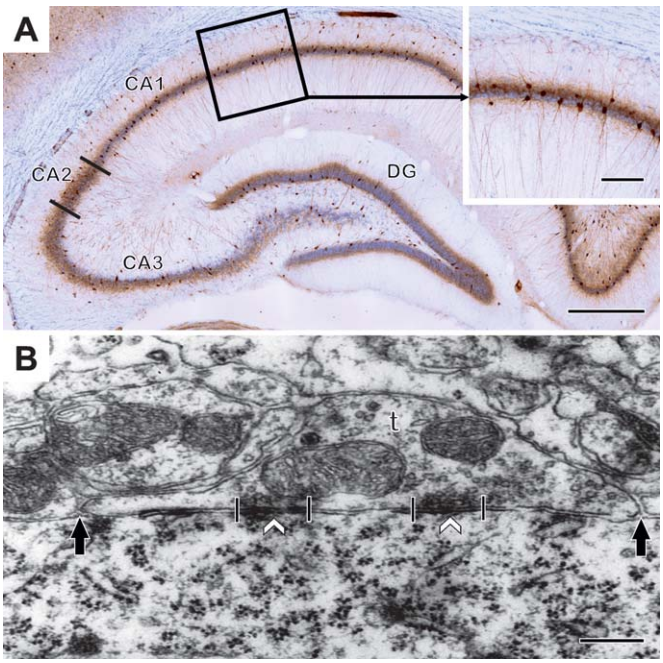


**FIGURE 4. A: A light microscopic image of a parvalbumin-immunostained preparation from the dorsal hippocampus. DG is the dentate gyrus, CA1-3 are regions of the Ammon's horn. Insert shows the outlined area of the CA1. This outlined area was used for the electron microscopic analysis. B: An electron micrograph of an axo-somatic terminal (t) in the CA1 area. The opposing length of the axon terminal (between the solid arrows), synapse length (between the crossing lines) and synapse numbers (white arrowheads) were measured and counted to compare the morphological features of perisomatic contacts and inhibitory synapses in the stressed and control animals. Scale bars: 0.5 mm on A; 0.125 mm on A insert; 250 nm on B. [Color figure can be viewed at wileyonlinelibrary.com]**

micrographs from the control and stressed animals are shown on Figure 5A,B. Since PV-immunoreactivity decreased substantially in the stressed animals and because most of the axon terminals were unlabeled thus, we investigated all axon terminals apposing to the somata of CA1 pyramidal cells. We analyzed 591 CA1 pyramidal neurons and 2538 perisomatic terminals in five control rats and 510 CA1 pyramidal neurons and 2307 perisomatic terminals in 4 stressed rats. Results of the systematic morphometric analysis of the perisomatic inhibitory synapses are shown on Tables 2 and 3. In the control rats, we observed the following values: The number of axon terminals was $10.1 \pm 0.5$ within 100 μm pyramidal cell perimeter. The number of terminals/soma was $4.2 \pm 0.2$ in the sections. We also estimated the number of terminals on a single CA1 pyramidal cell surface and this number was $56.6 \pm 4.3$. The average soma perimeter was $41.8 \pm 1.9$ μm and the average terminal length was $920.1 \pm 24.5$ nm. The synapse/terminal ratio was $32.1 \pm 0.7\%$ and we found $119.6 \pm 2.2$ synapses in 100 terminals. These axo-somatic parameters of the stressed animals were very similar to the control values (Tables 2 and 3). Nine weeks of stress had no detectable effect on any of these parameters. Furthermore, in our ultrastructural analysis we did not find any indication of neuronal degeneration or cell death in the hippocampi of the stressed animals. In our samples both the PV+ cell bodies (Fig. 5C) and their axon terminals (Fig. 5D) appeared to be normal in the stressed animals. We did not quantify the frequency of PV+ axon terminals, because we have used deeper ultrathin sections from the block where the immunoreaction was already weak, but the quality of ultrastructure was better. Since our aim was to determine the number of axo-somatic synapses in general, we did not count separately the PV+ terminals. They were part of our quantification.

## DISCUSSION

To our best of knowledge this is the first study to examine perisomatic inhibitory synapses in the hippocampi of rats subjected to long term stress. We used the chronic mild stress (CMS) model, which is one of the best described and validated animal models for depression, and analyzed the number and morphology of axo-somatic inhibitory synapses in the hippocampal CA1 area. Long term stress had no effect on the density and morphology of the perisomatic inhibitory synapses despite the significantly reduced density of perisomatic inhibitory PV+ neurons in the light microscopic preparations and the depressive-like behavior of the animals. This finding is in sharp contrast to the pronounced remodeling of the excitatory spine synapses in response to stress or depressive-like behavior which have been repeatedly shown in the literature (Magarinos et al., 1997; Sandi et al., 2003; Pawlak et al., 2005; Stewart et al., 2005; Donohue et al., 2006; Hajszan et al., 2009; Sousa et al., 2000; Maras et al., 2014). A likely explanation for this difference is the fact that axo-somatic synapses are stable structures compared to the axo-spinous synapses since spines are highly plastic structures, they may grow or disappear rapidly under various circumstances. Changes in spine numbers and spinous synapses have been documented in other pathological conditions, e.g. epilepsy, hypoxia/ischemia, as well as under physiological circumstances like the estrous cycle or memory formation and consolidation, or after antidepressant drug treatment (Gould et al., 1990; Woolley and McEwen, 1992; Okada et al., 1993; Norrholm and Ouimet, 2001; Jourdain at el., 2002; Hajszan et al., 2005).

The light microscopic observation that stress can decrease the number of PV+ neurons has two possible explanations: either the PV+ neurons die as a result of stress-induced neurotoxicity, or the PV content of the cells is reduced below the level of immuno-detection. Our hypothesis was that if the PV+ neurons would die in response to stress then, this should also affect the number of perisomatic synapses as well. We could not confirm this however. Our present data showing intact perisomatic inhibitory synapses in the chronically stressed animals suggest that the PV+ neurons do not die instead they only reduce their PV content. We should also

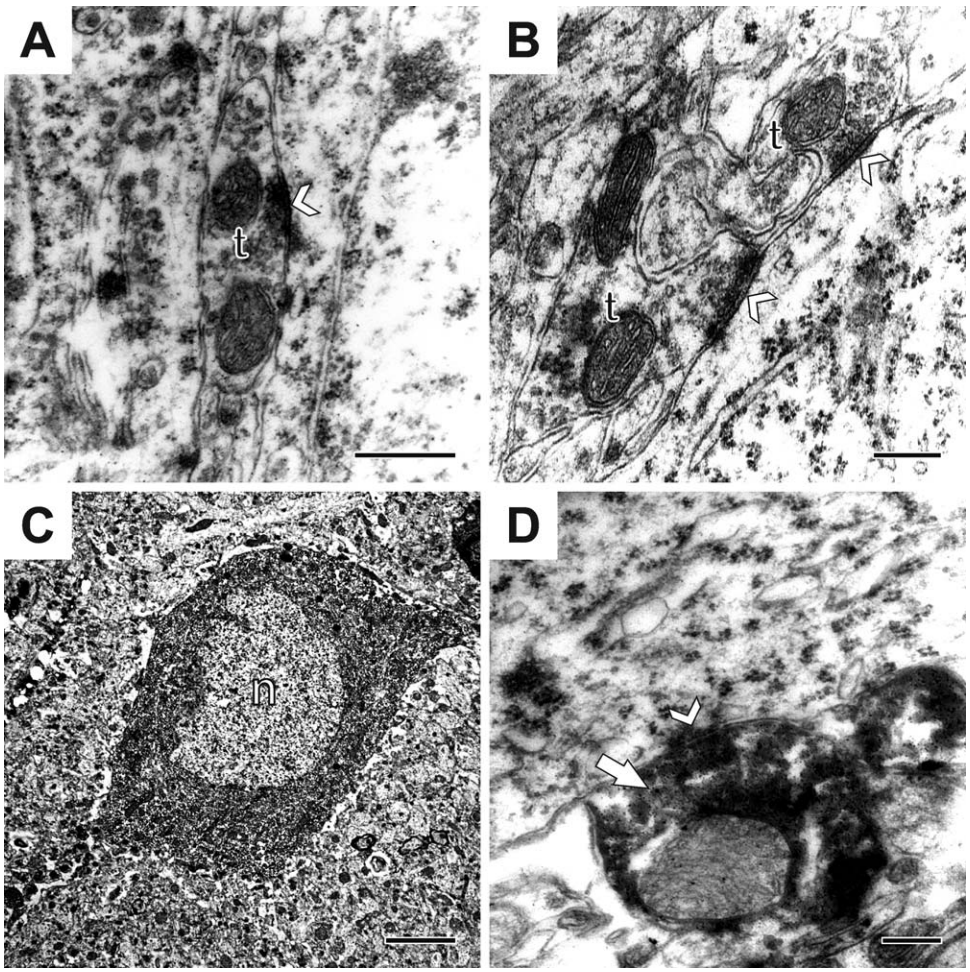


**FIGURE 5. Electron micrographs from control (A) and stressed rats (B). (A): An axon-terminal (t) with an axo-somatic synapse (white arrowhead) between two pyramidal neurons in the hippocampal CA1 region of a control rat. Occasionally such terminals formed synapses with both pyramidal cells. (B): Two axon-terminals (t) opposing a pyramidal neuron in a stressed animal. Synapses are indicated by white arrowheads. (C): A parvalbumin-positive neuron (n) inside the pyramidal layer of the CA1 showing the normal features as infolded nucleus and a large cytoplasm with abundant cytoplasmic organelles. (D): A parvalbumin-positive axon-terminal (white arrow) with an axo-somatic synapse (white arrowhead). Scale bars: 400nm on A; 200nm on B; 5μm on C and 400nm on D. Abbreviations: axon-terminal (t); nucleus (n).**

emphasize that during our ultrastructural analysis, where we examined 510 CA1 pyramidal neurons in four stressed animals, we did not find any indication of neuronal degeneration or cell death in the stressed animals.

A number of studies documented that long term stress can reduce PV+ interneuron numbers in all hippocampal subareas in the light microscopic preparations (Czéh et al., 2005, 2015; Harte et al., 2007; Hu et al., 2010; Schiavone et al., 2012; Filipovic et al., 2013; Milner et al., 2013; Godavarthi et al., 2014; Megahed et al., 2015). Furthermore, one of these earlier studies also reported on neuronal degeneration and death in the hilar region of the chronically stressed rats, indicating that PV+ neurons may die in response to chronic stress (Milner et al., 2013). Our present data suggest that the PV+ perisomatic inhibitory neurons do not die, instead they only reduce their PV-content and thus, they are not detectable with PV-immunohistochemistry anymore. It should be pointed out that regional differences may also exist. Since the Milner et al. (2013) study investigated the hilar region whereas, we examined the CA1 area thus, it could be that PV+ neurons are lost in the hilus, but remain in the CA1. Alternatively, the cell degeneration that was found in the hilus by Milner et al. (2013) was in fact affecting the hilar mossy cells. The glutamatergic mossy cells are present in the hilus in large numbers and they are known to be sensitive to any noxious stimuli (Scharfman, in press). Notably, in the hilus only 20% of the neurons are GABA-ergic (Czéh et al., 2013).

It should be pointed out that reduced PV-content after injury have been documented in another CNS disorder. In the epileptic hippocampus, basket cells can lose their PV-immunoreactivity, while the neurons are not lost (Sloviter et al., 2003). For example Scotti and co-workers studied

*TABLE 2.*

*Individual Data of Perisomatic Inhibitory Synapse Numbers and Morphology*

| | Control # 1 | Control # 2 | Control # 3 | Control # 4 | Control # 5 | Stress # 1 | Stress # 2 | Stress # 3 | Stress # 4 |
|---|---|---|---|---|---|---|---|---|---|
| Number of analyzed CA1 pyramidal neurons | 177 | 101 | 101 | 106 | 106 | 124 | 111 | 160 | 115 |
| Number of analyzed terminals | 886 | 420 | 394 | 425 | 413 | 578 | 497 | 779 | 453 |
| Number of terminals/soma cross section | 5.0 ± 0.1 | 4.2 ± 0.2 | 3.9 ± 0.2 | 4.0 ± 0.2 | 3.9 ± 0.1 | 4.7 ± 0.2 | 4.5 ± 0.2 | 4.9 ± 0.1 | 3.9 ± 0.1 |
| Number of terminals/100 μm cell perimeter | 11.3 ± 0.4 | 9.9 ± 0.6 | 9.2 ± 0.6 | 8.9 ± 0.5 | 11.3 ± 0.4 | 10.1 ± 0.4 | 10.4 ± 0.5 | 10.3 ± 0.4 | 11.4 ± 0.5 |
| Estimated number of terminals/soma | 70.5 ± 2.8 | 56.4 ± 1.7 | 53.8 ± 1.5 | 58.8 ± 2.3 | 43.7 ± 1.4 | 69.3 ± 2.2 | 63.0 ± 2.6 | 73.9 ± 3.2 | 42.9 ± 1.2 |
| Average soma perimeter (micrometer) | 44.2 ± 0.8 | 41.9 ± 0.6 | 43.2 ± 0.6 | 45.0 ± 1.0 | 34.6 ± 0.6 | 46.4 ± 0.6 | 42.9 ± 1.0 | 47.3 ± 1.0 | 34.6 ± 0.5 |
| Synapse/terminal ratio (%) | 31.7 | 32.4 | 34.3 | 32.5 | 29.9 | 36.2 | 36.0 | 29.0 | 32.97 |
| Synapse number/100 terminal | 124.5 | 117.8 | 119.1 | 112.7 | 123.8 | 116.5 | 127.8 | 117.9 | 115.7 |
| Average terminal length (nanometer) | 980.9 ± 27.3 | 977.2 ± 36.4 | 868.6 ± 22.7 | 877.2 ± 28.8 | 896.8 ± 30.3 | 889.1 ± 38.8 | 941.6 ± 38.8 | 955.5 ± 36.3 | 807.2 ± 25.1 |

Note the minimal differences between the individual rats. Data are expressed as mean ± S.E.M.

epilepsy models and demonstrated that in the CA1 PV-immunoreactivity disappeared while the GABAergic neurons survived (Scotti et al., 1997a,b). Similar data has been shown in biopsy brain tissue from epileptic patients. There, the surviving CA1 pyramidal neurons received intact perisomatic inhibitory input and the basket and axo-axonic cells survived, although many of them lost their PV-immunoreactivity (Wittner et al., 2005).

The exact physiological function of the calcium-binding protein parvalbumin is not clear. It has been shown that PV content within the neurons modulates the $Ca^{2+}$-dependent release of GABA (Vreugdenhil et al, 2003). In case of chronic stress, the sustained stress-induced glutamate release (Moghaddam, 1993; Popoli et al., 2011) and the consequent over-excitation of the PV+ neurons most probably disrupts their calcium buffering systems (Hu et al., 2010). Most probably the persistently elevated $Ca^{2+}$ level in the PV+ cells is detrimental to their cellular integrity and by that chronic stress causes functional and structural deficits in PV+ cells. Furthermore, about 50% of the fronto-cortical PV+ neurons express glucocorticoid receptors which suggest that stress has a direct effect on them (McKlveen et al., in press). Functional impairment of the PV-containing basket cells should result in deficits of GABA mediated rhythmic activity of the hippocampal network. It has been shown, that if PV+ neurons are lost from the neuronal circuitry that weakens the coordinated neuronal activity (Lodge

*TABLE 3.*

*Group Values of the Quantitative Ultrastructural Analysis*

| | **Control group ($n = 5$)** | **Stress group ($n = 4$)** | ***t*-Test analysis** |
|---|---|---|---|
| Number of analyzed CA1 pyramidal neurons | 118 ± 14.7[a] | 128 ± 11.2 [a] | $t=0.52$, $P=0.62$ |
| Number of analyzed terminals | 507 ± 94.9[a] | 577 ± 72.2[a] | $t=0.56$, $P=0.59$ |
| Number of terminals/soma cross section | 4.2 ± 0.2 | 4.5 ± 0.2 | $t=1.05$, $P=0.33$ |
| Number of terminals/100 μm cell perimeter | 10.1 ± 0.5 | 10.5 ± 0.3 | $t=0.64$, $P=0.54$ |
| Estimated number of terminals/Soma surface | 56.6 ± 4.3 | 62.3 ± 6.8 | $t=0.74$, $P=0.48$ |
| Average soma perimeter (micrometer) | 41.8 ± 1.9 | 42.8 ± 2.9 | $t=0.30$, $P=0.77$ |
| Synapse/terminal ratio (%) | 32.1 ± 0.7 | 33.6 ± 1.7 | $t=0.89$, $P=0.40$ |
| Synapse number/100 terminal | 119.6 ± 2.2 | 119.5 ± 2.8 | $t=0.02$, $P=0.98$ |
| Average terminal length (nanometer) | 920.1 ± 24.5 | 898.3 ± 33.6 | $t=0.54$, $P=0.61$ |

There was no difference between the Control and Stress groups in any of the parameters. In the statistical analysis '*n*' was the number of animals.
[a]In total, we analyzed 591 CA1 pyramidal neurons and 2538 perisomatic terminals in five control rats and 510 CA1 pyramidal neurons and 2307 perisomatic terminals in four stressed rats. Data are expressed as mean ±S.E.M.

et al., 2009). In harmony with that, we have documented that in animals that were subjected to chronic stress capacity of PV+ neurons to generate rhythmic oscillations is impaired (Hu et al., 2010). Similarly to our earlier data a recent study demonstrated that early life stress can also disrupt the maturation of the gamma oscillation network (Dricks, 2016), which was most probably the consequent of the impaired functioning of the PV+ basket cell network which is fundamental to gamma oscillations. Another study reported that chronic stress can shift the GABA reversal potential in the hippocampus and by that increases seizure susceptibility (MacKenzie and Maguire, 2015). In addition to that we have repeatedly demonstrated disturbed GABAergic transmission in the hippocampi of chronically stressed rats. We found increased frequency of spontaneous inhibitory postsynaptic currents (sIPSCs) in the CA1 area (Hu et al., 2010), whereas in the dentate gyrus, the frequency of sIPSCs was reduced (Holm et al., 2011). We also documented an impairment of CB1-mediated short-term plasticity of GABAergic synapses in chronically stressed animals (Hu et al., 2011).

Finally, we should add that our present report also provides further quantitative information on axo-somatic terminals and synapses in the control hippocampal CA1 area. To our best of knowledge there are only two reports which describe quantitative analysis of inhibitory synapses in the rodent hippocampus. Megías and co-workers (2001) investigated and quantified the distribution and total number of inhibitory (and excitatory) synapses on CA1 pyramidal cells. They found that a single pyramidal neuron receives around 30,000 excitatory and 1700 inhibitory inputs. Furthermore, 40% of the inhibitory input is located at the perisomatic region and that only inhibitory inputs innervate the somata (77-103 per cell) and axon initial segments (Megías et al., 2001). In a follow-up study, the same group demonstrated that a CA1 pyramidal cell body receives synapses from about 60 synaptic terminals in the CA1 and about 60% of these terminals are PV+, whereas 35-40% of them are CB1+ (type 1 cannabinoid receptor positive) (Takács et al., 2015). Our ultrastructural analysis had a somewhat different approach, since we were more interested in potential group differences, while the above mentioned studies focused more on the precise neuroanatomy of the inhibitory synapses. Still, the data are comparable, for example our finding on 40-70 terminals/soma is very similar to the 50–70 terminals/soma which have been reported by Takács et al. (2015).

In conclusion, the present data show that 9-weeks of daily stress reduced number of PV+ neurons in light microscopic preparations, but had no effect on the perisomatic inhibitory synapses. This is in sharp contrast to the remarkable remodeling of the excitatory synapses on spines that has been reported in response to stress and depressive-like behavior.

## ACKNOWLEDGMENTS

The authors have no conflict of interest to declare.

## REFERENCES

Czéh B, Simon M, van der Hart MG, Schmelting B, Hesselink MB, Fuchs E. 2005. Chronic stress decreases the number of parvalbumin-immunoreactive interneurons in the hippocampus: prevention by treatment with a substance P receptor (NK1) antagonist. Neuropsychopharmacology 30:67–79.

Czéh B, Abrahám H, Tahtakran S, Houser CR, Seress L. 2013. Number and regional distribution of GAD65 mRNA-expressing interneurons in the rat hippocampal formation. Acta Biol Hung 64: 395–413.

Czéh B, Varga ZK, Henningsen K, Kovács GL, Miseta A, Wiborg O. 2015. Chronic stress reduces the number of GABAergic interneurons in the adult rat hippocampus, dorsal-ventral and region-specific differences. Hippocampus 25:393–405.

Dricks S. 2016. Effects of neonatal stress on gamma oscillations in hippocampus. Sci Rep 6:29007-

Donohue HS, Gabbott PL, Davies HA, Rodríguez JJ, Cordero MI, Sandi C, Medvedev NI, Popov VI, Colyer FM, Peddie CJ, Stewart MG. 2006. Chronic restraint stress induces changes in synapse morphology in stratum lacunosum-moleculare CA1 rat hippocampus: a stereological and three-dimensional ultrastructural study. Neuroscience 140:597–606.

Duman RS. 2014. Pathophysiology of depression and innovative treatments: Remodeling glutamatergic synaptic connections. Dialogues Clin Neurosci 16:11–27.

Filipovic D, Zlatkovic J, Gass P, Inta D. 2013. The differential effects of acute vs. chronic stress and their combination on hippocampal parvalbumin and inducible heat shock protein 70 expression. Neuroscience 236:47–54.

Freund TF, Buzsáki G. 1996. Interneurons of the hippocampus. Hippocampus 6:347–470.

Freund TF, Katona I. 2007. Perisomatic inhibition. Neuron 56:33–42.

Gould E, Woolley CS, Frankfurt M, McEwen BS. 1990. Gonadal steroids regulate dendritic spine density in hippocampal pyramidal cells in adulthood. J Neurosci 10:1286–1291.

Gronli J, Fiske E, Murison R, Bjorvatn B, Sorensen E, Ursin R, Portas CM. 2007. Extracellular levels of serotonin and GABA in the hippocampus after chronic mild stress in rats. A microdialysis study in an animal model of depression. Behav Brain Res 181:42–51.

Godavarthi SK, Sharma A, Jana NR. 2014. Reversal of reduced parvalbumin neurons in hippocampus and amygdala of Angelman syndrome model mice by chronic treatment of fluoxetine. J Neurochem 130:444–454.

Hajszan T, MacLusky NJ, Leranth C. 2005. Short-term treatment with the antidepressant fluoxetine triggers pyramidal dendritic spine synapse formation in rat hippocampus. Eur J Neurosci 21: 1299–1303.

Hajszan T, Dow A, Warner-Schmidt JL, Szigeti-Buck K, Sallam NL, Parducz A, Leranth C, Duman RS. 2009. Remodeling of hippocampal spine synapses in the rat learned helplessness model of depression. Biol Psychiatry 65:392–400.

Harte MK, Powell SB, Swerdlow NR, Geyer MA, Reynolds GP. 2007. Deficits in parvalbumin and calbindin immunoreactive cells in the hippocampus of isolation reared rats. J Neural Transm (Vienna) 114:893–898.

Henningsen K, Andreasen JT, Bouzinova EV, Jayatissa MN, Jensen MS, Redrobe JP, Wiborg O. 2009. Cognitive deficits in the rat chronic mild stress model for depression: relation to anhedonic-like responses. Behav Brain Res 198:136–141.

Henningsen K, Palmfeldt J, Christiansen S, Baiges I, Bak S, Jensen ON, Gregersen N, Wiborg O. 2012. Candidate hippocampal biomarkers of susceptibility and resilience to stress in a rat model of depression. Mol Cell Proteomics 11:M111 016428.

Holm MM, Nieto-Gonzalez JL, Vardya I, Henningsen K, Jayatissa MN, Wiborg O, Jensen K. 2011. Hippocampal GABAergic dysfunction in a rat chronic mild stress model of depression. Hippocampus 21:422–433.

Hu W, Zhang M, Czéh B, Flügge G, Zhang W. 2010. Stress impairs GABAergic network function in the hippocampus by activating nongenomic glucocorticoid receptors and affecting the integrity of the parvalbumin-expressing neuronal network. Neuropsychopharmacology 35:1693–1707.

Hu W, Zhang M, Czéh B, Zhang W, Flügge G. 2011. Chronic restraint stress impairs endocannabinoid mediated suppression of GABAergic signaling in the hippocampus of adult male rats. Brain Res Bull 85:374–379.

Jourdain P, Nikonenko I, Alberi S, Muller D. 2002. Remodeling of hippocampal synaptic networks by a brief anoxia-hypoglycemia. J Neurosci 22:3108–3116.

Kallarackal AJ, Kvarta MD, Cammarata E, Jaberi L, Cai X, Bailey AM, Thompson SM. 2013. Chronic stress induces a selective decrease in AMPA receptor-mediated synaptic excitation at hippocampal temporoammonic-CA1 synapses. J Neurosci 33:15669–15674.

Kosaka T, Katsumaru H, Hama K, Wu JY, Heizmann CW. 1987. GABAergic neurons containing the Ca2+-binding protein parvalbumin in the rat hippocampus and dentate gyrus. Brain Res 419: 119–130.

Krugers HJ, Lucassen PJ, Karst H, Joëls M. 2010. Chronic stress effects on hippocampal structure and synaptic function: relevance for depression and normalization by anti-glucocorticoid treatment. Front Synaptic Neurosci 2:24-

Lee V, MacKenzie G, Hooper A, Maguire J. Reduced tonic inhibition in the dentate gyrus contributes to chronic stress-induced impairments in learning and memory. Hippocampus (in press). [Epub ahead of print] doi: 10.1002/hipo.22604.

Leuner B, Shors TJ. 2013. Stress, anxiety, and dendritic spines: What are the connections?. Neuroscience 251:108–119.

Lodge DJ, Behrens MM, Grace AA. 2009. A loss of parvalbumin-containing interneurons is associated with diminished oscillatory activity in an animal model of schizophrenia. J Neurosci 29:2344–2354.

Lucassen PJ, Pruessner J, Sousa N, Almeida OF, Van Dam AM, Rajkowska G, Swaab DF, Czéh B. 2014. Neuropathology of stress. Acta Neuropathol 127:109–135.

MacKenzie G, Maguire J. 2013. Neurosteroids and GABAergic signaling in health and disease. Biomol Concepts 4:29–42.

MacKenzie G, Maguire J. 2015. Chronic stress shifts the GABA reversal potential in the hippocampus and increases seizure susceptibility. Epilepsy Res 109:13–27.

Magarinos AM, McEwen BS, Flügge G, Fuchs E. 1996. Chronic psychosocial stress causes apical dendritic atrophy of hippocampal CA3 pyramidal neurons in subordinate tree shrews. J Neurosci 16: 3534–3540.

Magarinos AM, Verdugo JM, McEwen BS. 1997. Chronic stress alters synaptic terminal structure in hippocampus. Proc Natl Acad Sci USA 94:14002–14008.

Maguire J. 2014. Stress-induced plasticity of GABAergic inhibition. Front Cell Neurosci 8:157-

Maras PM, Molet J, Chen Y, Rice C, Ji SG, Solodkin A, Baram TZ. 2014. Preferential loss of dorsal-hippocampus synapses underlies memory impairments provoked by short, multimodal stress. Mol Psychiatry 19:811–822.

Markram H, Toledo-Rodriguez M, Wang Y, Gupta A, Silberberg G, Wu C. 2004. Interneurons of the neocortical inhibitory system. Nat Rev Neurosci 5:793–807.

McEwen BS, Bowles NP, Gray JD, Hill MN, Hunter RG, Karatsoreos IN, Nasca C. 2015. Mechanisms of stress in the brain. Nat Neurosci 18:1353–1363.

McKlveen JM, Morano RL, Fitzgerald M, Zoubovsky S, Cassella SN, Scheimann JR, Ghosal S, Mahbod P, Packard BA, Myers B, Baccei ML, Herman JP. Chronic stress increases prefrontal inhibition: A mechanism for stress-induced prefrontal dysfunction. Biol Psychiatry (in press). Mar 28. pii:S0006-3223(16)32234-X. doi: 10.1016/j.biopsych.2016.03.2101. [Epub ahead of print]

Megahed T, Hattiangady B, Shuai B, Shetty AK. 2015. Parvalbumin and neuropeptide Y expressing hippocampal GABA-ergic inhibitory interneuron numbers decline in a model of Gulf War illness. Front Cell Neurosci 8:447.

Megías M, Emri Z, Freund TF, Gulyás AI. 2001. Total number and distribution of inhibitory and excitatory synapses on hippocampal CA1 pyramidal cells. Neuroscience 102:527–540.

Milner TA, Burstein SR, Marrone GF, Khalid S, Gonzalez AD, Williams TJ, Schierberl KC, Torres-Reveron A, Gonzales KL, McEwen BS, Waters EM. 2013. Stress differentially alters mu opioid receptor density and trafficking in parvalbumin-containing interneurons in the female and male rat hippocampus. Synapse 67:757–772.

Mody I, Maguire J. 2012. The reciprocal regulation of stress hormones and GABA(A) receptors. Front Cell Neurosci 6:4-

Moghaddam B. 1993. Stress preferentially increases extraneuronal levels of excitatory amino acids in the prefrontal cortex: comparison to hippocampus and basal ganglia. J Neurochem 60:1650–1657.

Norrholm SD, Ouimet CC. 2001. Altered dendritic spine density in animal models of depression and in response to antidepressant treatment. Synapse 42:151–163.

Okada R, Nishizuka M, Iizuka R, Arai Y. 1993. Persistence of reorganized synaptic connectivity in the amygdala of kindled rats. Brain Res Bull 31:631–635.

Pawlak R, Rao BS, Melchor JP, Chattarji S, McEwen B, Strickland S. 2005. Tissue plasminogen activator and plasminogen mediate stress-induced decline of neuronal and cognitive functions in the mouse hippocampus. Proc Natl Acad Sci USA 102:18201–18206.

Paxinos G, Watson C. 1998. The Rat Brain in Stereotaxic Coordinates. San Diego, CA: Academic Press.

Popoli M, Yan Z, McEwen BS, Sanacora G. 2011. The stressed synapse: The impact of stress and glucocorticoids on glutamate transmission. Nat Rev Neurosci 13:22–37.

Ribak CE, Nitsch R, Seress L. 1990. Proportion of parvalbumin-positive basket cells in the GABAergic innervation of pyramidal and granule cells of the rat hippocampal formation. J Comp Neurol 300:449–461.

Sandi C, Davies HA, Cordero MI, Rodriguez JJ, Popov VI, Stewart MG. 2003. Rapid reversal of stress induced loss of synapses in CA3 of rat hippocampus following water maze training. Eur J Neurosci 17:2447–2456.

Scharfman HE. The enigmatic mossy cell of the dentate gyrus. Nat Rev Neurosci (in press). doi: 10.1038/nrn.2016.87. [Epub ahead of print]

Schiavone S, Jaquet V, Sorce S, Dubois-Dauphin M, Hultqvist M, Bäckdahl L, Holmdahl R, Colaianna M, Cuomo V, Trabace L, Krause KH. 2012. NADPH oxidase elevations in pyramidal neurons drive psychosocial stress-induced neuropathology. Transl Psychiatry 2:e111-

Scotti AL, Bollag O, Kalt G, Nitsch C. 1997a. Loss of perikaryal parvalbumin immunoreactivity from surviving GABAergic neurons in the CA1 field of epileptic gerbils. Hippocampus 7:524–535.

Scotti AL, Kalt G, Bollag O, Nitsch C. 1997b. Parvalbumin disappears from GABAergic CA1 neurons of the gerbil hippocampus with seizure onset while its presence persists in the perforant path. Brain Res 760:109–117.

Sloviter RS, Zappone CA, Harvey BD, Bumanglag AV, Bender RA, Frotscher M. 2003. "Dormant basket cell" hypothesis revisited: Relative vulnerabilities of dentate gyrus mossy cells and inhibitory interneurons after hippocampal status epilepticus in the rat. J Comp Neurol 459:44–76.

Sousa N, Lukoyanov NV, Madeira MD, Almeida OF, Paula-Barbosa MM. 2000. Reorganization of the morphology of hippocampal neurites and synapses after stress-induced damage correlates with behavioral improvement. Neuroscience 97:253–266.

Stewart MG, Davies HA, Sandi C, Kraev IV, Rogachevsky VV, Peddie CJ, Rodriguez JJ, Cordero MI, Donohue HS, Gabbott PL, Popov VI. 2005. Stress suppresses and learning induces plasticity in CA3 of rat hippocampus: a three-dimensional ultrastructural study of thorny excrescences and their postsynaptic densities. Neuroscience 131:43–54.

Takács VT, Szőnyi A, Freund TF, Nyiri G, Gulyás AI. 2015. Quantitative ultrastructural analysis of basket and axo-axonic cell terminals in the mouse hippocampus. Brain Struct Funct 220:919–940.

Timmermans W, Xiong H, Hoogenraad CC, Krugers HJ. 2013. Stress and excitatory synapses: from health to disease. Neuroscience 248: 626–636.

Thompson SM, Kallarackal AJ, Kvarta MD, Van Dyke AM, LeGates TA, Cai X. 2015. An excitatory synapse hypothesis of depression. Trends Neurosci 38:279–294.

Vreugdenhil M, Jefferys JG, Celio MR, Schwaller B. 2003. Parvalbumin-deficiency facilitates repetitive IPSCs and gamma oscillations in the hippocampus. J Neurophysiol 89:1414–1422.

Watanabe Y, Gould E, McEwen BS. 1992. Stress induces atrophy of apical dendrites of hippocampal CA3 pyramidal neurons. Brain Res 588:341–345.

Whissell PD, Cajanding JD, Fogel N, Kim JC. 2015. Comparative density of CCK- and PV-GABA cells within the cortex and hippocampus. Front Neuroanat 9:124-

Wiborg O. 2013. Chronic mild stress for modeling anhedonia. Cell Tissue Res 354:155–169.

Willner P. 2005. Chronic mild stress (CMS) revisited: consistency and behaviouralneurobiological concordance in the effects of CMS. Neuropsychobiology 52:90–110.

Willner P, Muscat R, Papp M. 1992. Chronic mild stress-induced anhedonia: a realistic animal model of depression. Neurosci Biobehav Rev 16:525–534.

Wittner L, Eross L, Czirják S, Halász P, Freund TF, Maglóczky Z. 2005. Surviving CA1 pyramidal cells receive intact perisomatic inhibitory input in the human epileptic hippocampus. Brain 128: 138–152.

Woolley CS, McEwen BS. 1992. Estradiol mediates fluctuation in hippocampal synapse density during the estrous cycle in the adult rat. J Neurosci 12:2549–2554.

Zaletel I, Filipovic D, Puskas N. 2016. Chronic stress, hippocampus and parvalbumin-positive interneurons: what do we know so far?. Rev Neurosci 27:397–409.